PAPER

Check for updates

An innovative study on the "on–off–on" detection of sulfur ions based on a TSPP–riboflavin fluorescent probe

Huan Wang, [ID] *[a] Wencheng Mu,[a] Yuanyuan Liu,[b] Yongchang Lu, [ID] [a] Yuang Qiu[a] and Qin Ma*[a]

In this paper, 5,10,15,20-(4-sulphonatophenyl) porphyrin (TSPP) was synthesized by a facile route and used as a fluorescent probe to construct a sensor system based on the high water solubility and high quantum yield. It was found that when riboflavin (RF) was introduced into the TSPP solution, the fluorescence intensity of TSPP decreased for the peaks at 645 nm and 700 nm based on the principle of the electrostatic attractions and hydrophobic interactions between TSPP and riboflavin. When the fluorescence emission peak of riboflavin appeared at 550 nm, the fluorescence sensor system changed from the "on" state to the "off" state. When sulfur ions (S^{2-}) were further introduced into the TSPP–riboflavin system, the fluorescence intensity of riboflavin was further decreased based on the specific reaction between S^{2-} and riboflavin. However, the fluorescence signal of TSPP was restored and the fluorescence sensing system changed from the "off" state to the "on" state. Therefore, TSPP was used as a fluorescent probe to construct an "on–off–on" fluorescent sensing system, the linear range of S^{2-} detected by this system is 5.0×10^{-9} to 3.6×10^{-5} M, and the detection limit (LOD) is 1.1×10^{-9} M. The sensing system has higher accuracy and sensitivity, and it can be successfully used in the sensing of S^{2-} in real samples.

Introduction

The sulfur ion (S^{2-}) is an extremely toxic pollutant,[1] which widely exists in natural water, domestic sewage, industrial waste water and biological systems. S^{2-} also causes a series of health problems owing to it having close association with living organisms in a variety of way.[2,3] Doing research about the detection of S^{2-} has become an important part of environment, human health and food safety for sustainable development.[4] Relevant medical research shows that free S^{2-} in biological systems is easily transformed into harmful hydrogen sulfide at physiological pH value. Also, it is well known that low concentrations of sulfur ions can cause dizziness, and high concentrations of S^{2-} can irritate the mucus in the cell membrane to cause suffocation,[5] cardiac arrest, diabetes[6] and other diseases. Therefore, it is urgent and necessary to find a simple, sensitive and fast method for S^{2-} detection.

Riboflavin, also known as vitamin B_2 (VB_2), is one of good water solubility in vitamin family, which plays an important role in living organisms.[7] In the organisms, the main physiological function of VB_2 is a coenzyme that can promote energy metabolism and biological oxidation–reduction processes, such as the metabolism of fat, carbohydrate and protein.[8] Adding RF into supplemental intake or adequate dietary will have biological protective effects in terms of anti-aging,[9] anti-inflammatory,[10] antioxidant,[11] and anticancer properties.[12] Generally speaking, excess or lack of RF is harmful to the normal metabolism of the organism. In addition to playing an important role in living organisms, RF is also a good fluorescent emitter, which is often used to construct various luminescent sensing systems based on good fluorescence properties.[13,14]

In recent years, porphyrins have been used as probes for fluorescent analysis in many fields of detection, such as anions, cations, neutral molecules, DNA, RNA, proteins, cells and viruses detection, *etc.* In 1990, Sessler first reported the method of anions detection based on porphyrins.[15] Lemon synthesized palladium porphyrins that was modified by quantum dot (QD), which improved the sensitivity of oxygen detected in organic solvents.[16] Fry detected mercury ions by mean of the spectroscopic method based on associating the porphyrin with a solid support.[17] Bu group have designed an on–off fluorescence sensor with high selectivity for cadmium(ii).[18] Lu group constructed various sensors based on porphyrin derivatives.[19,20] Beyene constructed a novel on–off colorimetric and fluorescent sensor of Cu^{2+}, Sn^{2+} and Zn^{2+} by water-soluble porphyrin.[21] In these porphyrin derivatives, sulfonated porphyrins have been

[a]Modern Tibetan Medicine Creation Engineering Technology Research Center of Qinghai Province, College of Pharmacy, Qinghai Nationalities University, China. E-mail: qhmuwh1028@126.com

[b]Yinchuan City Center for Disease Control and Prevention, Ningxia, China
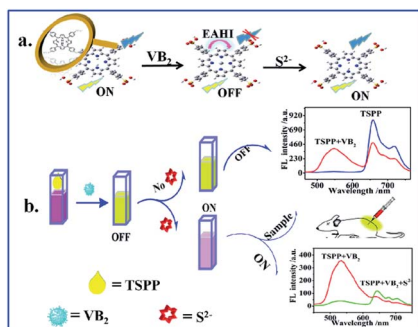
Fig. 1 Schematic illustration of the principle of the sensor system.

widely used in molecular recognition, fluorescence analysis,[22] electrochemistry,[23] drug therapy,[24,25] electrochemiluminescence (ECL),[26] photoelectrochemical sensor[27] and other fields because of their excellent water-soluble, physical and chemical properties. However, up to now, the fluorescence detection method of S^{2-} based on 5,10,15,20-sulfonic acid phenyl porphyrin–riboflavin (TSPP–VB_2) fluorescence probe has not been reported.

In this study, the physical characteristics of VB_2 exhibit strong yellow green fluorescence under ultraviolet radiation, and its chemical characteristics can react with S^{2-} specifically. The "on–off–on" fluorescence probe of TSPP–VB_2 system is successfully constructed in this experimental environment, and its working principle is as shown in Fig. 1. TSPP at 645 nm has strong fluorescence under 460 nm excitation wavelength, which can be explained that the fluorescence signal of the fluorescence sensing system is the "on" state. When different concentrations of VB_2 are introduced into TSPP solution, the fluorescence intensity of TSPP is gradually quenched due to the electrostatic attractions and hydrophobic interactions between VB_2 and TSPP. With the increase of VB_2 concentration, the fluorescence intensity of VB_2 becomes progressively stronger especially at 550 nm, and the fluorescence intensity of TSPP in the sensing system changes from "on" to "off". When a certain concentration of S^{2-} is continually introduced into the TSPP–VB_2 system, the fluorescence intensity of VB_2 is gradually weakened owing to the specific reaction between VB_2 and S^{2-}. While the fluorescence signal of TSPP is restored, the fluorescence sensing system is restored to the "on" state.

Experimental

Reagents

$NaHCO_3$ and Tris used in this experiment were all purchased from Yantai Shuangshuang Chemical Co., Ltd. Concentrated sulfuric acid (H_2SO_4, 98%) purchased from Baishi Reagent Company. Pyrrole, benzaldehyde, methanol, chloroform and propionic acid were purchased from Energy Chemical Reagent Company. The deionized water (18.25 m Ω) used in the experiment was prepared by ultra pure water mechanism in the laboratory. The other reagents were pure for analysis and were not further purified before their use, and all experiments were conducted at room temperature.

Instrument

The fluorescence spectra were obtained through Cary Eclipse Fluorescence Analyzer (Agilent Technologies, USA). Ultraviolet-visible absorption spectra were collected in a TU-1901 spectrophotometer (Beijing's General Instrument Limited Company, Beijing, China); Fourier transform infrared spectra (FT-IR) spectra were recorded on an IR Prestige 21 (Shimadzu, Tokyo, Japan). The concentrated samples were collected through a rotary evaporator (BUCHI Labortechnik AG, Switzerland). Vacuum drying of samples were used for a DZF-6020 vacuum drying oven (Yuhua Instrument Co., Ltd., China). The pH of the samples were tested on a pHS-3B pH meter (Shanghai Precision Instrument Science Co., China).

Synthesis of 5,10,15,20-tetraphenyl porphyrin (TPP) and 5,10,15,20-(4-sulfonic acid) tetraphenyl porphyrin (TSPP)

Synthesis of 5,10,15,20-tetraphenyl porphyrins (TPP). 5,10,15,20-Tetraphenylporphyrin (TPP) was synthesized according to the "one pot method" reported in the literature.[28] The process is as the following: 250 mL propionic acid is added into a 500 mL three-necked round-bottom flask, which is heated by an oil bath to a slight boiling point, and then 10 mL benzaldehyde is added into it, 7 mL freshly steamed pyrrole is dissolved into 30 mL propionic acid that is slowly dropped into the reaction bottle. After the process above, the flask is needed to stop heating after the reflux for 1 h, and cool it to room temperature and rest overnight in the refrigerator. The reaction liquid above is vacuumed and filtered later, the filter residue is washed by anhydrous ethanol and water for 2–3 times respectively, and then dried to get purple solid. The samples were mixed and purified by silica gel column chromatography. The eluents were the volume ratio of 3 : 1 of the dichloromethane and petroleum ether. The final product was obtained about 4 g, and the 58% product was gotten by steaming and drying.

Synthesis of 5,10,15,20-(4-sulphonatophenyl) porphyrins (TSPP). The TSPP is synthesized according to the method reported in previous literature.[22] The specific process is as follows: 200 mg of TPP above is added into 100 mL single neck round bottom flask, which is dissolved by a small amount of chloroform. 10 mL of concentrated H_2SO_4 is further slowly added into the mixture above, which is needed to be heated to 91 °C with magnetic stirring, and then green clear solution is obtained after its reflux for 4 h at constant temperature. Cooling the solution to room temperature later, the saturated $NaHCO_3$ solution is slowly added to obtain the purple solution. The solution is filtered after cooling in ice water bath, and the precipitation is dissolved by 150 mL methanol, and then filtered. The above steps are repeated for 2–3 times, and the recrystallization of propanol is added. Next, the purple solid is obtained by filtering, and then the solid is needed to be dried in vacuum. The final product gotten is 53 mg with a yield of 32.4%.

Preparation of solutions

The preparation of Tris–HCl buffer solution (pH = 8). 100 mL (0.10 M) trimethylol aminomethane solution (Tris) and

proper (0.10 M) hydrochloric acid solution were prepared, respectively. Then, the two kinds of solution were mixed together according to a certain volume ratio to obtain the different pH values of Tris–HCl solution. The pH value is measured by a pH meter, therefore, different pH values of Tris–HCl buffer solution was obtained in this experiment.

The preparation of fluorescent probe TSPP reserve solution. The prepared TSPP powder of 0.4 mg was accurately weighed and dissolved by a small amount of deionized water, and then putting it into a 100 mL volumetric flask that was needed to fixed the volume by the deionized water. As a result, the TSPP reserve solution with a concentration of 0.5 μM was obtained.

Fluorescence detection of sulfur ions (S^{2-})

At room temperature, the process of fluorescence detection of S^{2-} based on TSPP–VB$_2$ fluorescent probe is as the following: 30 μL (0.5 μM) TSPP stock solution and 1 mL (0.10 M, pH = 8) Tris–HCl buffer solution were taken into the 2 mL sample tube, and 50 μL (1 mM) VB$_2$ solution is added into the above solution. Then, fresh S^{2-} solution with different concentrations were separately mixed into the TSPP–VB$_2$ system. Finally, 2 mL sample tube is fixed to the scale by the deionized water, and then shaking up it well. After incubating for about 5 min, the changes of fluorescence intensity of TSPP–VB$_2$ solution were detected under the condition of the excitation wavelength of 460 nm and slit width of 5 × 5 nm.

Real sample preparation

1 mL of blood was obtained from the ear of a rabbit, and it was placed in a centrifuge tube at room temperature for 4 h and refrigerated for 12 h. The upper layer of serum was removed in an ultraclean hood, centrifuged at 4000 rpm for 15 min. After the process of preparation above, the serum was collected. It was processed by the aseptic method, and then refrigerated until analysis.

4 g milk was accurately weighed and putted into a 10 mL colorimetric tube, and then acetonitrile was also fixed to the scale above. After 15 min of ultrasonic extraction, the sample was placed in a refrigerator at 4 °C for 10 min to precipitate the protein, and centrifuged at 8000 rpm for 20 min. Next, 1 mL supernatant was blow-dried with nitrogen at 60 °C, and placed in a 10 mL colorimetric tube that is fixed to the scale with ultrapure water. The diluted solution was filtered through the 0.22 μm organic filter membrane and degreaser column. After the processing above, the filtrate were obtained and used as the stock solution for the analysis of real sample.

5 mL beverage solution was centrifuged at 5000 rpm for 10 min, and the supernatant was filled with ultrapure water to 50 mL colorimetric tube. The diluent above was passed through SPE-C$_{18}$ solid phase extraction column. The first 1 mL of the liquid was discarded and 5 mL of the filtrate from the back was collected. The filtrate was passed through nylon 0.22 μm microporous membrane, and the filtrate was used as the stock solution for the analysis.

Results and discussion

UV-vis absorption and fluorescence emission spectra

The optical properties of the synthesized TSPP were detected by UV-vis absorption and fluorescence emission spectra in Fig. 2. It can be seen from the UV-vis absorption spectra (red line in Fig. 2) that there are 5 absorption peaks in total, among which the peak with the larger absorbance value at 415 nm is the B absorption band, also which is known as Soret band and is the characteristic absorption peak of porphyrins. The other four absorption peaks with relatively small absorbance values are Q absorption bands with absorption wavelengths of 514 nm, 551 nm, 579 nm and 631 nm, respectively. As the fluorescence emission spectra (green line in Fig. 2) showed that the TSPP solution presented two obvious fluorescence emission peaks at 645 nm and 700 nm under the excitation wavelength of 460 nm. The inner illustration shows the photograph information of TSPP solution under sunlight lamp (left) and red fluorescence was irradiated with the UV lamp at 365 nm (right).

FT-IR spectrum analysis

The Fourier transform infrared spectra (FT-IR) of synthetic TSPP is as shown in Fig. 3, 1445 cm^{-1} is the stretching vibration absorption peak of C=C on the benzene ring and porphyrin ring; the absorption peak at 2580–2940 cm^{-1} is the C–H stretching vibration absorption peak on the typical aromatic ring; 1609 cm^{-1} and 1667 cm^{-1} are the stretching vibration
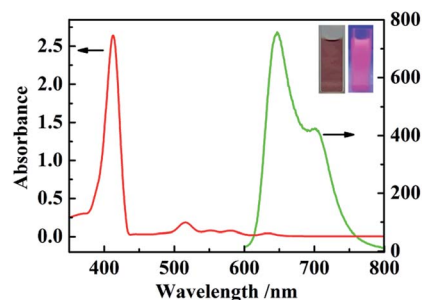

Fig. 2 The UV-vis absorption (red line), fluorescence emission spectra (green line) under the 460 nm excitation wavelength. The interior illustration shows the picture in visible light (left) and the fluorescent image of a TSPP solution under 365 nm UV light (right) (the concentration of TSPP dispersion was 38 μM).
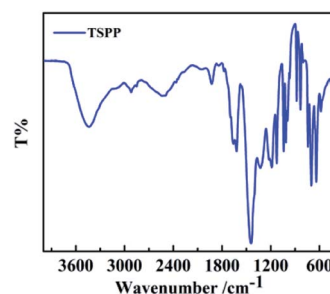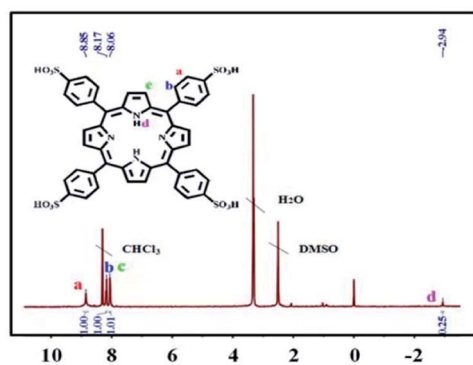

Fig. 3 FT-IR spectrum of TSPP.

Fig. 4 ^{1}H NMR spectrum of TSPP.

absorption peaks of N=C on the benzene ring and porphyrin ring; and 1650 cm^{-1} is the stretching vibration of C–O. In addition, the characteristic absorption peaks of sulfonic acid groups are 1179 cm^{-1}, 1129 cm^{-1} and 638 cm^{-1}, respectively.

1 H NMR spectrum analysis

The TSPP powder of vacuum drying was accurately weighed, which is dissolved by DMSO solvent, and then the mixture is added into the nuclear magnetic tube. The experiment of ^{1}H NMR was carried out by using tetramethylsilane (TMS) as internal standard. The chemical displacement values of the compound measured in the experiment are as shown in Fig. 4. The details of the ^{1}H NMR obtained are as follows: ^{1}H NMR (400 MHz, DMSO-d$_6$) δ, ppm: 8.85(s, 8H), 8.17(d, 8H, J = 4.0 Hz), 8.06(d, 8H, J = 8.0 Hz), −2.94(s, 2H).

Effect of VB$_2$ concentration on fluorescence intensity of TSPP solution

The relationship between VB$_2$ concentration and fluorescence intensity of TSPP is as shown in Fig. 5. The fluorescence intensity of TSPP solution gradually decreased with the addition of VB$_2$ solution. When the concentration of VB$_2$ increased to 2.5 × 10^{-5} M, the fluorescence intensity of TSPP solution decreased to the lowest level. The fluorescence intensity of TSPP solution did not decrease significantly when the concentration of VB$_2$
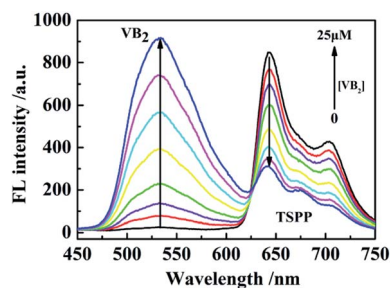
continued to increase. Therefore, the fluorescent probe is constructed with 25 μM VB$_2$ solution in this experiment.

Selection of experimental conditions

It is well known that both the reaction time and the pH value of buffer solution have a certain effect on the fluorescence intensity of fluorophore. Therefore, in this study, the effect of different pH values in Tris–HCl buffer solution and the reaction time between TSPP–VB$_2$ and S^{2-} on the fluorescence signal at 550 nm were investigated by using the fluorescence signal peak of VB$_2$ as a reference. The relationship between the pH of 0.1 M Tris–HCl buffer solution and the fluorescence intensity of TSPP–VB$_2$ system is as shown in Fig. 6A. With the increase of pH value, the fluorescence intensity of TSPP–VB$_2$ system changes constantly. When the pH value is 8, the maximum fluorescence intensity of the system is about 650 a.u., so the optimal pH value of Tris–HCl buffer solution is 8. When a certain concentration of S^{2-} solution was added into the mixed system, the change of fluorescence intensity of TSPP–VB$_2$ system with the time changing is as shown in Fig. 6B. With the extension of reaction time, the fluorescence intensity of the system decreases continuously, but when it reaches 5 min, it almost no longer decreases as the extension of reaction time. Therefore, 5 min was selected as the optimal response time of the system in this experiment.

Fluorescence detection S^{2-}

Fig. 7 shows the relationship between the fluorescence intensity of TSPP–VB$_2$ solution and S^{2-} concentration. As is illustrated in Fig. 7A, with the increase of S^{2-} concentration, the fluorescence intensity of VB$_2$ decreases gradually at 550 nm, and the fluorescence intensity of TSPP increases gradually at 645 nm. The recovery rate of fluorescence intensity of TSPP at 645 nm is relatively weak, while the degree of decrease of fluorescence intensity of VB$_2$ at 550 nm is relatively obvious. Therefore, the fluorescence signal peak of VB$_2$ at 550 nm is used as a reference peak to fit the linear relationship in this sensor research. As is shown in Fig. 7B, it can be seen that the fluorescence intensity of TSPP–VB$_2$ solution has a linear relationship with the increase of S^{2-} concentration. The linear fitting curve equation is: $Y = -182.4 \log[\text{S}^{2-}] + 310.4$ ($R^2 = 0.9975$), the linear range of S^{2-} detection is 5.0 × 10^{-9} to 3.6 × 10^{-5} M, and the detection limit (LOD) is calculated to be 1.10 × 10^{-9} M by 3δ/k (where δ was the blank standard deviation; k was the slope of the linear fitting

Fig. 5 The fluorescence intensity of TSPP varies with the concentration of VB$_2$ (from bottom to top, the concentrations of VB$_2$ were 0 to 25 μM).
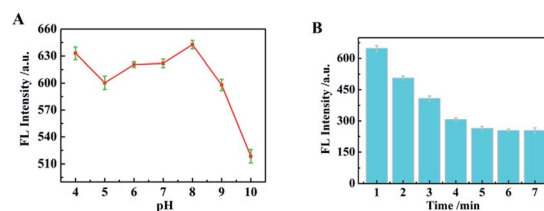

Fig. 6 (A) Fluorescence intensity of TSPP–VB$_2$ system at different pH values; (B). Relationship between fluorescence intensity and incubation time of TSPP–VB$_2$–S^{2-}.
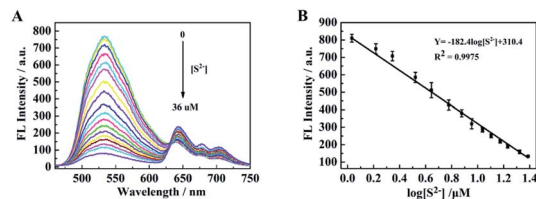
Fig. 7 (A) Fluorescence emission spectra of TSPP–VB$_2$ system with increasing concentration of S^{2-}. (B) Relationship between fluorescence intensity of TSPP and the concentration of VB$_2$.

Fig. 8 Fluorescence response of the TSPP–VB$_2$ system toward S^{2-} and the different interfering substances (the concentrations of other interfering substances were about 1000 times than the concentration of S^{2-}).

Table 1 Comparison of different methods for S^{2-} sensing

Fluorescent probes	Detection limit (μM)	Linear range (μM)	Ref.
g-CNQDs–ZnMOF	15×10^{-3}	0.005–1.0	29
L–Cu^{2+}	0.14	0.5–10	30
CdS QDs	1.6	7–125	31
Tyloxapol/MnO$_4^-$	0.039	130–200	32
g-C$_3$N$_4$–Ag$^+$	3.5×10^{-3}	0–0.03	33
Papain-directed AuNCs	80	0.2–20	34
CDs/PEI/NB	0.06	0.1–8	35
Fe$_3$O$_4$@SiO$_2$	0.12	0–12	36
TSPP–VB$_2$	1.10×10^{-3}	0–36	This work

Table 2 Determination of S^{2-} by TSPP in serum, milk and beverage

Sample	Added (10^{-7} M)	Found (10^{-7} M)	Recovery (%)	RSD (%, $n = 3$)
Serum	0.25	0.24	97.33	6.28
	3.50	3.55	101.52	5.69
	65.00	65.25	100.38	6.70
Milk	0.25	0.26	102.67	5.95
	3.50	3.36	96.00	2.73
	65.00	63.42	97.56	5.39
Beverage	0.25	0.24	97.47	6.23
	3.50	3.66	104.57	6.40
	65.00	61.59	94.75	4.23

curve equation). Compared with other detection systems (Table 1), the fluorescence sensing system constructed in this experiment has higher accuracy and sensitivity.

Selective test of S^{2-} by TSPP–VB$_2$ fluorescence

The selectivity of the sensor directly determines whether the system can be applied in practice. Therefore, the selectivity for the determination of S^{2-} was characterized. When other interfering substances are added into TSPP–VB$_2$ solution, the change of fluorescence intensity of TSPP–VB$_2$ solution is as shown in Fig. 8, where F_0 and F are the fluorescence intensities of VB$_2$ in the absence and presence of S^{2-}. The interferents selected in this experiment were CO$_3^{2-}$, F$^-$, NO$_3^-$, I$^-$, Cl$^-$, SO$_4^{2-}$, lysine, phenylalanine, methionine, cysteine, GSH, Mg^{2+} and Ca^{2+}(the concentration of the interfering substances is about 1000 times than the concentration of S^{2-}). The fluorescence intensity of TSPP–VB$_2$ changed when a certain concentration of interfering substances were added, but the fluorescence intensity did not decrease significantly. Consequently, the TSPP–VB$_2$ fluorescent probe molecule constructed in this experiment has a good selectivity for the detection of S^{2-}.

Detection of S^{2-} content in actual samples

In order to further prove that the TSPP–VB$_2$ fluorescent probe constructed in this research can be successfully applied to the detection of S^{2-} in actual samples, the content of S^{2-} in the actual samples (rabbit serum, milk and beverage) was determined by the method of adding standard. The experimental results are as shown in Table 2. The recovery rate and relative standard deviation (RSD) of S^{2-} in the actual samples were
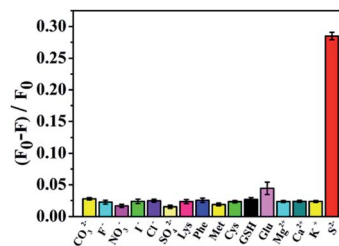
between the range of 94.75–104.57% and 2.73–6.70%, respectively. It can be clearly seen that this method can be well applied to the detection of S^{2-} content in the actual samples.

Discussion the detection mechanism

In this "on–off–on" fluorescence sensing research, TSPP acts as a fluorescent emitter. When VB$_2$ is introduced into TSPP solution, it produces its own fluorescence at 550 nm, and the fluorescence intensity of TSPP was weakened at 645 nm owing to that VB$_2$ is also a special fluorescent luminescent group. The interaction between TSPP solution and VB$_2$ is as shown in Fig. 9. As can be seen from the experimental results in Fig. 9, sulfur ions have almost no effect on the fluorescence intensity of TSPP without VB$_2$. Sulfur ions can weaken the fluorescence intensity of VB$_2$ based on the specific interaction between VB$_2$ and S^{2-} in the absence of TSPP. Thereof, TSPP and VB$_2$ may exists the interacting relationship conducted in this study based on the principle of the electrostatic attractions and hydrophobic interactions from TSPP to riboflavin.

It was found that when S^{2-} was further introduced into the TSPP–VB$_2$ system, the fluorescence signal of VB$_2$ decreased linearly. On the contrary, the fluorescence intensity of TSPP gradually recovered, which indicated that there was a specific reaction between S^{2-} and VB$_2$. According to previous reports, sulfur ions mainly exist in the form of HS$^-$ in buffer solutions with pH = 8.[37] In this experiment, the decrease of fluorescence intensity of VB$_2$ maybe the results of the reaction between the triplet state of riboflavin (^{3}VB$_2^*$) and HS$^-$.[38] In order to further study the interaction mechanism between them above, the UV-
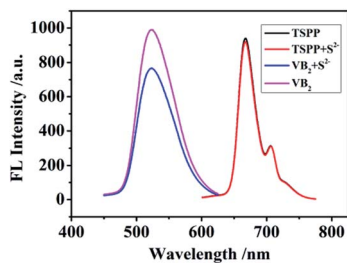
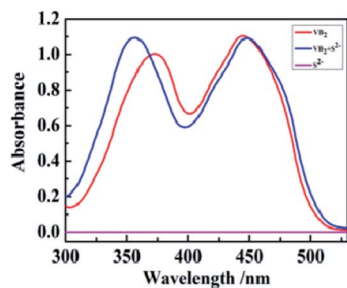Fig. 9 Fluorescence emission spectra of TSPP, VB_2, the mixture of TSPP and S^{2-}, the mixture of VB_2 and S^{2-}.

Fig. 10 UV-vis absorption spectra of VB_2, S^{2-} and the mixture of VB_2 and S^{2-}.

vis absorption spectra of S^{2-}, VB_2 and mixtures of S^{2-}–VB_2 are seriously studied in this paper, as is shown in Fig. 10. It can be seen from the research results that when S^{2-} and VB_2 are mixed together, the blue shift of UV-vis absorption peak at 370 nm can be observed obviously. This could be due to that the main S^{2-} and the molecular structure of the VB_2 amide groups have a special interaction. This interaction can make S^{2-} destroy the ring structure in VB_2 molecular structure, which results in the decrease of unsaturation of molecular structure. Also, it causes that the UV-vis absorption peak at 370 nm moves towards the short wave direction. Based on this mechanism, the "on–off–on" fluorescent probe was constructed to study the sensing of S^{2-} in the real samples.

Conclusion

First and foremost of all, the synthesis method of TSPP reported was successfully improved in this study, which makes the synthesis of TSPP greener, and the yield was increased by about 10%. Also, TSPP was further characterized by various spectra. What's more, the detection of S^{2-} of the "on–off–on" fluorescent sensor based on TSPP–VB_2 was successfully constructed. In addition, the optimal reaction conditions of the sensor system were optimized, and interference experiments were studied. Last but not least, the content of S^{2-} in rabbit serum, milk and beverage was respectively detected by the method of adding standard. The research above shows that the "on–off–on" fluorescence detection system constructed in this experiment can selectively detect S^{2-} in actual samples. Compared with the detection method of pure porphyrin compound probe, the method in this study can better improves the sensitivity of

detection, and has the remarkable advantages of low price, simple operation and less time. So this research method has the bright and good prospect in the fields of the sensing research, and it is worth of popularizing in the practical application.

Conflicts of interest

There are no conflicts to declare.

Notes and references

1 X. Pang, L. Wang, L. Gao, H. Feng, J. Kong and L. Li, *Luminescence*, 2019, **34**, 585–594.
2 F. Cheng, X. Wu, M. Liu, Y. Lon, G. Chen and R. Zeng, *Sens. Actuators, B*, 2016, **228**, 673–678.
3 N. Kumar, V. Bhalla and M. Kumar, *Coord. Chem. Rev.*, 2013, **257**, 2335–2347.
4 S. Wang, L. Wang, Y. Zhu and Y. Song, *Spectrochim. Acta, Part A*, 2020, **236**, 118327.
5 Y. Jia, Y. Guo, S. Wang, W. Chen, J. Zhang, W. Zheng and X. Jiang, *Nanoscale*, 2017, **9**, 9811–9817.
6 H. Wang, X. Wu, S. Yang, H. Tian, Y. Liu and B. Sun, *Dyes Pigm.*, 2019, **160**, 757–764.
7 H. Wang, Q. Ma, Y. Wang, C. Wang, D. Qin, D. Shan, J. Chen and X. Lu, *Anal. Chim. Acta*, 2017, **973**, 34–42.
8 T. Tabanlıgil Calam, *Microchem. J.*, 2021, **169**, 106557.
9 Y. Zou, M. Ruan, J. Luan, X. Feng, S. Chen and Z. Chu, *J. Nutr., Health Aging*, 2017, **21**, 314–319.
10 A. I. Mazur, J. Natorska, E. Wypasek, E. Kołaczkowska and B. Płytycz, *Cent. Eur. J. Immunol.*, 2008, **33**, 98–101.
11 A. Masek, E. Chrzescijanska, M. Zaborski and M. Maciejewska, *C. R. Chim.*, 2012, **15**, 524–529.
12 N. Suwannasom, I. Kao, A. Pru, R. Georgieva and H. Bumler, *Int. J. Mol. Sci.*, 2020, **21**, 950.
13 Z. Wang, L. Zhang, Y. Hao, W. Dong and X. Gong, *Anal. Chim. Acta*, 2021, **1144**, 1–13.
14 S. Feng, F. Pei, Y. Wu, J. Lv and W. Lei, *Spectrochim. Acta, Part A*, 2021, **246**, 119004.
15 J. L. Sessler, M. J. Cyr, V. Lynch, E. McGhee and J. A. Ibers, *J. Am. Chem. Soc.*, 1990, **112**, 2810–2813.
16 C. M. Lemon, E. Karnas, M. G. Bawendi and D. G. Nocera, *Inorg. Chem.*, 2013, **52**, 10394–10406.
17 D. Fry and M. Zamadar, *Res. Rev.: J. Chem.*, 2015, **4**, 46–55.
18 Q. Zhao, R. Li, S. Xing, X. Liu, T. Hu and X. Bu, *Inorg. Chem.*, 2011, **50**, 10041–10046.

© 2022 The Author(s). Published by the Royal Society of Chemistry

19 D. Zhang, P. Du, J. Chen, H. Guo and X. Lu, *Sens. Actuators, B*, 2021, **341**, 130000.

20 L. Li, X. Ning, Y. Qian, G. Pu, Y. Wang, X. Zhang, H. Wang, J. Chen, D. Shan and X. Lu, *Sens. Actuators, B*, 2017, **257**, 331–339.

21 B. Beyene, A. Ybeltal and M. Ayana, *Results Chem.*, 2020, **2**, 100058.

22 J. Chen, Q. Ma, X. Hu, Y. Gao, X. Yan, D. Qin and X. Lu, *Sens. Actuators, B*, 2018, **254**, 475–482.

23 Y. Zeng, J. Liu and Y. Li, *Electrochem. Commun.*, 2002, **4**, 679–683.

24 S. Simionescu, S. Teodorescu, R. M. Ion and G. Nechifor, *Mater. Plast.*, 2016, **53**, 194–197.

25 R. M. Ion and S. Patachia, in *International Conference on Advancements of Medicine and Health Care through Technology*, Cluj-Napoca, Romania, 2014, vol. 44, pp. 307–310.

26 J. Zhang, S. Devaramani, D. Shan and X. Lu, *Anal. Bioanal. Chem.*, 2016, **408**, 7155–7163.

27 M. Xi, P. Wang, M. Zhang, L. Qin, S. Z. Kang and X. Li, *Appl. Surf. Sci.*, 2020, **529**, 147200.

28 J. Chen, Y. Gao, Q. Ma, X. Hu, Y. Xu and X. Lu, *Sens. Actuators, B*, 2018, **268**, 270–277.

29 Y. Pan, X. Xu, Y. Zhang, Y. Zhang and W. Dong, *Spectrochim. Acta, Part A*, 2020, **229**, 117927.

30 L. Hou, X. Kong, Y. Wang, J. Chao, C. Li, C. Dong, Y. Wang and S. Shuang, *J. Mater. Chem. B*, 2017, **5**, 8957–8966.

31 P. Sianglam, S. Kulchat, T. Tuntulani and W. Ngeontae, *Spectrochim. Acta, Part A*, 2017, **183**, 408–416.

32 P. Ding, X. Xin, L. Zhao, Z. Xie, Q. Zhang, J. Jiao and G. Xu, *RSC Adv.*, 2017, **7**, 3051–3058.

33 S. Wang, D. Du, M. Yang, Q. Lu, R. Ye, X. Yan and Y. Lin, *Talanta*, 2017, **168**, 168–173.

34 L. C. Wang, G. Q. Chen, G. M. Zeng, J. Liang, H. R. Dong, M. Yan, Z. W. Li, Z. Guo, W. Tao and L. Peng, *New J. Chem.*, 2015, **39**, 9306–9312.

35 H. Jin, R. J. Gui, Y. F. Wang and J. Sun, *Talanta*, 2017, **169**, 141–148.

36 H. Jiang, Y. Liu, W. Luo, Y. Wang, X. Tang, W. Dou, Y. Cui and W. Liu, *Anal. Chim. Acta*, 2018, **1014**, 91–99.

37 J. R. Koenitzer, T. S. Isbell, H. D. Patel, G. A. Benavides and D. W. Kraus, *Am. J. Physiol.: Heart Circ. Physiol.*, 2007, **292**, 1953–1960.

38 M. Wang, K. Li, R. R. Zhu, L. L. Cheng, Q. S. Wu and S. L. Wang, *J. Photochem. Photobiol., B*, 2011, **103**, 186–191.